

A new sequence of hierarchic prismatic elements satisfying De Rham diagram on hybrid meshes

P. ŠOLÍN*, K. SEGETH†

Received

Received in revised form

Communicated by

Abstract — This paper presents a new sequence of affine-equivalent $H(\text{curl})$ - and $H(\text{div})$ -conforming hierarchic prismatic finite elements of arbitrary polynomial degrees, satisfying De Rham diagram on hybrid tetrahedral-prismatic-hexahedral meshes. We also present suitable $H(\text{curl})$ - and $H(\text{div})$ -conforming reference maps that preserve the commutativity of the De Rham diagram.

Keywords: prismatic elements, higher-order elements, hierarchic elements, hp -FEM, hybrid meshes, De Rham diagram

1. INTRODUCTION

In the early era of the finite element approximation of the Maxwell's equations it was assumed that the right space for the discretization of the electric field E was $[H^1(\Omega_h)]^d$. It was observed, however, that globally continuous discretizations lead to spurious waves and other unwanted phenomena (see, e.g., [9,10,16]). Today it is understood that finite element subspaces of $[H^1(\Omega_h)]^d$ cannot form Galerkin sequences in the much larger space $H(\text{curl}, \Omega_h)$ – see, e.g., [3]. The discovery of this fact motivated the development of discontinuous vector-valued elements conforming to the space $H(\text{curl}, \Omega_h)$. Since both in 2D and 3D the degrees of freedom on the lowest-order $H(\text{curl}, \Omega_h)$ -conforming elements were associated with the element edges, these elements were named *edge elements*.

The lowest-order edge elements were first introduced by Whitney [18] in a different context of geometrical integration theory. They were independently rediscovered and applied to the Maxwell's equations by several authors (see, e.g., [1,4,5]). In the 1980s the edge elements have been developed mainly in the nodal framework (Nédélec elements [12,11]). Hierarchic edge ($H(\text{curl})$) and face ($H(\text{div})$) elements appeared more recently (see, e.g., [2,14,17]) due to the rapid development of the hp -FEM in the last years. These results concerned elements of Cartesian geometries

This work was supported by the Czech Science Foundation Grants 102/05/0629 and 201/04/1503, and by the Academy of Sciences of the Czech Republic Institutional Research Plan AV0Z10190503.

*Department of Mathematical Sciences, The University of Texas at El Paso, El Paso, TX

†Mathematical Institute, Academy of Sciences of the Czech Republic, Prague

(quadrilaterals and hexahedra) and simplicial geometries (triangles and tetrahedra). In the present paper we complete them by deriving suitable arbitrary-order prismatic edge and face elements, that can be used to connect the arbitrary-order tetrahedral and hexahedral elements in hybrid meshes.

It is well-known that there is a strong connection between the good behavior of edge and face elements and the commuting properties of the De-Rahm diagram. The 3D version of the diagram has the form

$$H^1 \xrightarrow{\nabla} H(\text{curl}) \xrightarrow{\nabla \times} H(\text{div}) \xrightarrow{\nabla \cdot} L^2. \quad (1.1)$$

For later reference, in the next Section 2 we mention the standard hierarchic prismatic element of arbitrary order for H^1 -conforming approximations. In Sections 3 and 4 we construct arbitrary-order hierarchic prismatic elements in the spaces $H(\text{curl})$ and $H(\text{div})$. In Section 5 the De Rham sequence is completed with arbitrary-order prismatic elements in the space L^2 . Last, for the sake of completeness, Section 6 discusses the $H(\text{curl})$ -, $H(\text{div})$ - and L^2 -conforming transformation relations of the master element shape functions into the physical mesh, as needed for algorithmic and implementation purposes.

2. H^1 -CONFORMING PRISMATIC ELEMENT \mathcal{K}_p^1

Let us choose a reference prismatic geometry in the product form $K_p = K_t \times K_a$,

$$K_p = \{\xi \in \mathbf{R}^3; -1 < \xi_1, \xi_2, \xi_3; \xi_1 + \xi_2 < 0; \xi_3 < 1\}, \quad (2.1)$$

where $K_t = ([-1, -1], [1, -1], [-1, 1])$ is a standard triangular reference domain and $K_a = (-1, 1)$ is a conventional one-dimensional reference interval. The reference prismatic domain K_p is shown in Figure 1.

One- and two-dimensional affine coordinates in the form

$$\begin{aligned} \lambda_{1,p}(\xi_1, \xi_2, \xi_3) &= \frac{\xi_2 + 1}{2}, \quad \lambda_{2,p}(\xi_1, \xi_2, \xi_3) = -\frac{\xi_1 + \xi_2}{2}, \\ \lambda_{3,p}(\xi_1, \xi_2, \xi_3) &= \frac{\xi_1 + 1}{2}, \quad \lambda_{4,p}(\xi_1, \xi_2, \xi_3) = \frac{\xi_3 + 1}{2}, \\ \lambda_{5,p}(\xi_1, \xi_2, \xi_3) &= \frac{1 - \xi_3}{2} \end{aligned} \quad (2.2)$$

will be used in the following.

In order to allow for anisotropic p -refinement of the prismatic elements, we assign two local directional orders of approximation $p^{b,1}, p^{b,2}$ to the element interior. The order $p^{b,1}$ corresponds to the plane $\xi_1 \xi_2$ (we will designate this the *planar direction*), and $p^{b,2}$ to the *vertical direction* ξ_3 . There are three quadrilateral faces $s_i, i = 1, \dots, 3$, which will be equipped with local directional orders of approximation $p^{s_i,1}, p^{s_i,2}$ (in planar and vertical direction, respectively). Triangular faces s_4, s_5

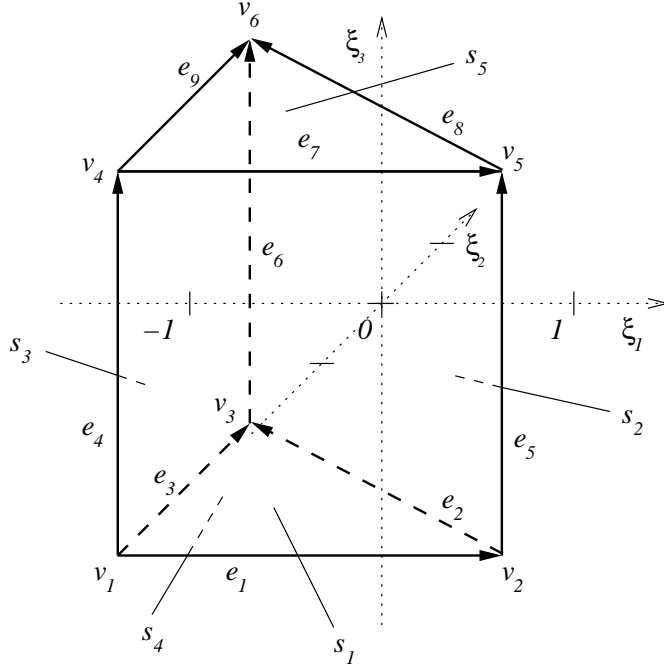


Figure 1. The reference prism K_P .

come with one local order of approximation p^{s_i} only, $i = 4, 5$, and local polynomial orders p^{e_1}, \dots, p^{e_9} are assigned to edges.

These local orders suggest that a finite element of the form $\mathcal{K}_P^1 = (K_P, W_P, \Sigma_P^1)$ will be assigned polynomial space

$$W_P = \left\{ w \in \mathcal{R}_{p^{b,1}, p^{b,2}}(K_P); w|_{s_i} \in \mathcal{Q}_{p^{s_i,1}, p^{s_i,2}}(s_i) \text{ for } i = 1, 2, 3; \right. \\ \left. w|_{s_i} \in \mathcal{P}_{p^{s_i}}(s_i) \text{ for } i = 4, 5; w|_{e_j} \in \mathcal{P}_{p^{e_j}}(e_j), j = 1, \dots, 9 \right\}. \quad (2.3)$$

Here

$$\mathcal{R}_{m_1, m_2}(K_P) = \text{span} \left\{ \xi_1^{n_1} \xi_2^{n_2} \xi_3^{n_3}; (\xi_1, \xi_2, \xi_3) \in K_t \times K_a; \right. \\ \left. 0 \leq n_1, n_2; n_1 + n_2 \leq m_1; 0 \leq n_3 \leq m_2 \right\}. \quad (2.4)$$

Vertex, edge, face and *bubble* functions will be used to define a suitable H^1 -hierarchic basis in the space W_P .

Vertex functions $\varphi_P^{v_j}$, $j = 1, 2, \dots, 6$, are associated with element vertices, and they provide a complete basis of W_P for lowest-order approximation. We define them as

$$\varphi_P^{v_j} = \lambda_{j_1, P} \lambda_{j_2, P}. \quad (2.5)$$

The indices j_1, j_2 correspond to the only two faces s_{j_1}, s_{j_2} of the reference prism K_P that *do not* contain the vertex v_j (recall that an affine coordinate is associated with the face where it entirely vanishes). In the standard sense, vertex functions $\varphi_P^{v_j}$ are equal to one at v_j and vanish at all remaining vertices. Their traces are linear on all edges. Construction of the vertex functions is illustrated in Figure 2.

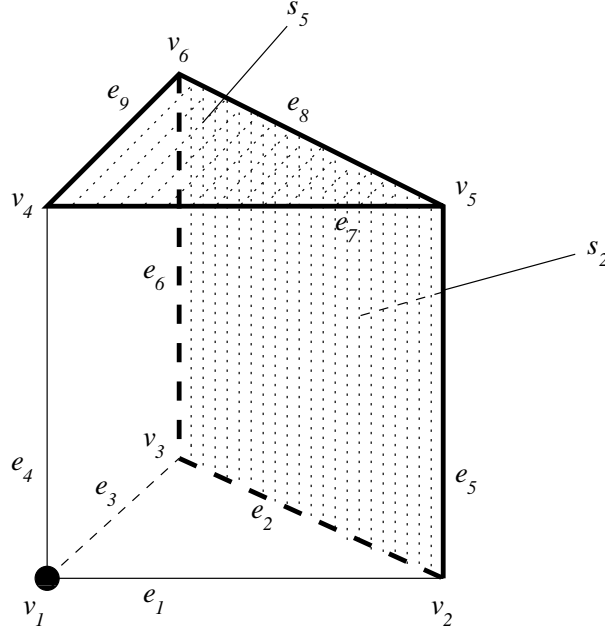


Figure 2. Vertex function $\varphi_P^{v_1}$ is equal to one at the vertex v_1 , and vanishes entirely on the faces s_2, s_5 . Thus it vanishes at all remaining vertices.

Edge functions $\varphi_{k,P}^{e_j}$, $j = 1, \dots, 9$, $k = 2, \dots, p^{e_j}$, will be designed to coincide with the *Lobatto shape functions* (integrated Legendre polynomials) $l_2, \dots, l_{p^{e_j}}$ on edges e_j , $j = 1, 2, \dots, 9$, and will vanish on all remaining edges. Let us choose an (oriented) edge $e_j = v_{i_1}v_{i_2}$. By s_{j_1}, s_{j_2} we denote the faces of the reference domain K_P that share a single vertex v_{i_1} or v_{i_2} with the edge e_j , respectively. Further by s_{j_3} we denote the only face of K_P that does not share any vertex with the edge e_j . We add to the basis of W_P (oriented) edge functions

$$\varphi_{k,P}^{e_j} = \lambda_{j_1,P} \lambda_{j_2,P} \varphi_{k-2}(\lambda_{j_1,P} - \lambda_{j_2,P}) \lambda_{j_3,P}, \quad 2 \leq k \leq p^{e_j}. \quad (2.6)$$

Construction of the edge functions is illustrated in Figure 3.

Triangular face functions, associated with faces s_i , $i = 4, 5$, will be designed to have on s_i a nonzero trace of local polynomial order k , $3 \leq k \leq p^{s_i}$, $1 \leq n_1, n_2$; $n_1 + n_2 = k - 1$, and will vanish on all remaining faces. First we equip each triangular face with a local orientation – we select three vertices $v_A, v_B, v_C \in s_i$ in such a way

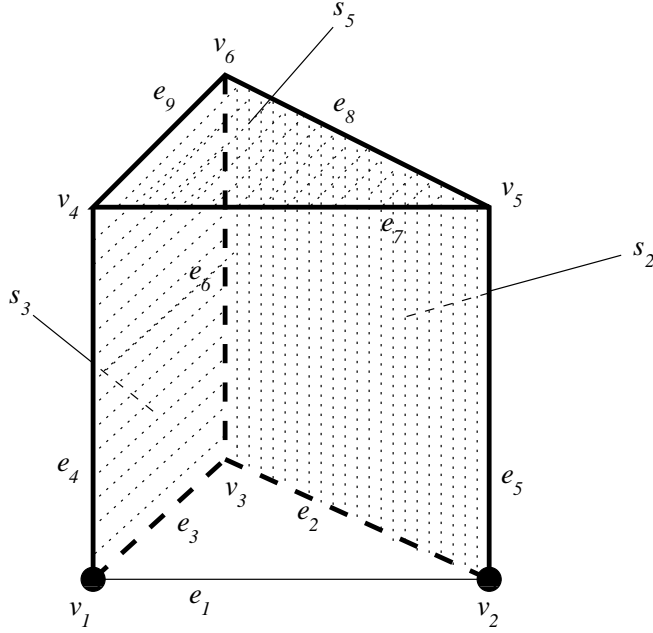


Figure 3. Traces of edge functions $\varphi_{n,p}^{e_1}$, $2 \leq n$, coincide with the Lobatto shape functions l_2, l_3, \dots on the edge e_1 , and vanish identically on all faces where the edge e_1 is not contained. Thus they also vanish along all remaining edges.

that v_A, v_C have the lowest and highest local index, respectively. For each face s_i we therefore have three affine coordinates $\lambda_A, \lambda_B, \lambda_C$, such that $\lambda_A(v_A) = \lambda_B(v_B) = \lambda_C(v_C) = 1$. By λ_D we denote affine coordinate corresponding to the other triangular face s_D , and write $(p^{s_i} - 2)(p^{s_i} - 1)/2$ face functions

$$\varphi_{n_1, n_2, T}^{s_i} = \lambda_A \lambda_B \lambda_C \varphi_{n_1-1}(\lambda_B - \lambda_A) \varphi_{n_2-1}(\lambda_A - \lambda_C) \lambda_D, \quad (2.7)$$

$1 \leq n_1, n_2; n_1 + n_2 \leq p^{s_i} - 1$.

Quadrilateral face functions, corresponding to faces s_i , $i = 1, \dots, 3$, will be constructed to have on s_i a trace of local directional polynomial orders n_1, n_2 , $2 \leq n_1 \leq p^{s_i,1}$, $2 \leq n_2 \leq p^{s_i,2}$, and will vanish on all remaining faces. Local coordinate axes on the faces are now chosen to share direction with the corresponding horizontal and vertical edges (see Figure 1).

There is a unique pair of edges belonging to the face s_i , both of which are parallel to the plane $\xi_1 \xi_2$. From this pair we select the (oriented) edge $e_j = v_{j_1} v_{j_2}$ belonging to the bottom face s_4 . Further, by s_{i_1}, s_{i_2} we denote the pair of faces that share a single vertex v_{j_1} or v_{j_2} with the edge e_j , respectively.

We can define face functions

$$\varphi_{n_1, n_2, P}^{s_i} = \lambda_{i_1, P} \lambda_{i_2, P} \lambda_{4, P} \lambda_{5, P} \varphi_{n_1-2}(\lambda_{i_1, P} - \lambda_{i_2, P}) \varphi_{n_2-2}(\lambda_{4, P} - \lambda_{5, P}), \quad (2.8)$$

$2 \leq n_1 \leq p^{s_i,1}$, $2 \leq n_2 \leq p^{s_i,2}$. The construction of face functions is illustrated in Figure 4.

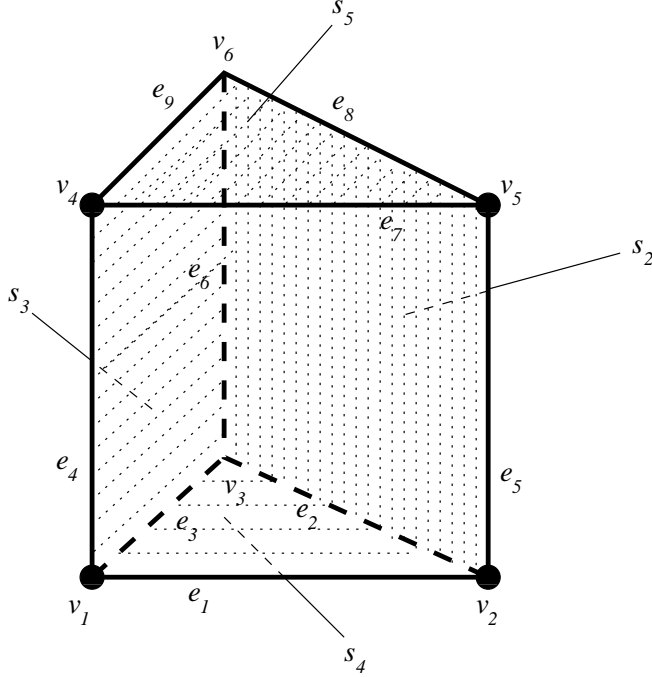


Figure 4. Quadrilateral face functions $\varphi_{n_1, n_2, p}^{s_1}$, $2 \leq n_1, n_2$ are nonzero on the face s_1 and in the element interior. They vanish on all faces except for s_1 and obviously on all edges and vertices as well.

Bubble functions vanish everywhere on the boundary of the reference domain. It will probably come as no surprise that we construct them as products of bubble functions corresponding to the master triangle \mathcal{K}_t^1 , and the Lobatto shape functions $l_2, l_3, \dots, l_{p^{b,2}}$ in $\tilde{\xi}_3$:

$$\varphi_{n_1, n_2, n_3, p}^b = \lambda_{1,p} \lambda_{2,p} \lambda_{3,p} \varphi_{n_1-1}(\lambda_{3,p} - \lambda_{2,p}) \varphi_{n_2-1}(\lambda_{2,p} - \lambda_{1,p}) l_{n_3}(\xi_3), \quad (2.9)$$

$1 \leq n_1, n_2$; $n_1 + n_2 \leq p^{b,1} - 1$; $2 \leq n_3 \leq p^{b,2}$. Hence the number of bubble functions is

$$(p^{b,1} - 2)(p^{b,1} - 1)(p^{b,2} - 1)/2. \quad (2.10)$$

Numbers of scalar hierarchic shape functions in the basis of the space W_P are summarized in Table 1.

Proposition 2.1. *Shape functions (2.5), (2.6), (2.7), (2.8), and (2.9) constitute a hierarchic basis of the space W_P , defined in (2.3).*

Table 1. Scalar hierarchic shape functions of \mathcal{K}_P^1 .

Node type	Polynomial order	Number of shape functions	Number of nodes
Vertex	always	1	6
Edge	$2 \leq p^{e_j}$	$p^{e_j} - 1$	9
Triangular face	$3 \leq p^{s_i}$	$(p^{s_i} - 2)(p^{s_i} - 1)/2$	2
Quadrilateral face	$2 \leq p^{s_{i,1}}, p^{s_{i,2}}$	$(p^{s_{i,1}} - 1)(p^{s_{i,2}} - 1)$	3
Interior	$3 \leq p^{b,1}, 2 \leq p^{b,2}$	(2.10)	1

Proof. Straightforward. □

Remark 2.1 Conditioning. When designing higher-order shape functions, the conditioning aspect becomes much more pronounced than in the lower-order case. It is well known that Lobatto shape functions are optimal in 1D (stiffness matrix for the Laplace operator with zero Dirichlet boundary conditions has the condition number equal to one). Bubble functions (2.9) were derived from the triangular shape functions

$$\varphi_{n_1, n_2, t}^b = \lambda_{1,P} \lambda_{2,P} \lambda_{3,P} \varphi_{n_1-1}(\lambda_{3,P} - \lambda_{2,P}) \varphi_{n_2-1}(\lambda_{2,P} - \lambda_{1,P}),$$

$1 \leq n_1, n_2; n_1 + n_2 \leq p^{b,1} - 1; 2 \leq n_3 \leq p^{b,2}$, first introduced in [13], [14]. Their conditioning was analyzed in [14] with favorable results.

3. $H(\text{CURL})$ -CONFORMING PRISMATIC ELEMENT $\mathcal{K}_P^{\text{CURL}}$

As in the scalar case, we allow for anisotropic p -refinement of prismatic elements, and therefore consider local directional orders of approximation $p^{b,1}, p^{b,2}$ in the interior. The order $p^{b,1}$ corresponds to the plane $\xi_1 \xi_2$ (we will designate this the *horizontal direction*) and $p^{b,2}$ to the *vertical direction* ξ_3 . We have three quadrilateral faces $s_i, i = 1, \dots, 3$, which will be equipped with local directional orders of approximation $p^{s_{i,1}}, p^{s_{i,2}}$ (in horizontal and vertical directions, respectively). Triangular faces s_4, s_5 come with one local order of approximation p^{s_i} per face only. Standard local polynomial orders p^{e_1}, \dots, p^{e_9} will be assigned to edges.

A finite element of arbitrary order on the reference domain K_P will be constructed in the conventional way as a triad $\mathcal{K}_P^{\text{curl}} = (K_P, Q_P, \Sigma_P^{\text{curl}})$. We saw in Section 2 that scalar polynomials φ on the reference prism $K_P = K_t \times K_a$ have a product form $\varphi \in \mathcal{R}_{m_1, m_2}(K_P)$, defined in (2.4). The way the gradient operator ∇ acts on a space of this form,

$$\mathcal{R}_{m_1+1, m_2+1}(K_P) \xrightarrow{\nabla} \mathcal{R}_{m_1, m_2+1}(K_P) \times \mathcal{R}_{m_1, m_2+1}(K_P) \times \mathcal{R}_{m_1+1, m_2}(K_P), \quad (3.1)$$

determines the choice of an appropriate ancestor space

$$W_P = \left\{ w \in \mathcal{R}_{p^{b,1}+1, p^{b,2}+1}(K_P); w|_{s_i} \in \mathcal{Q}_{p^{s_i,1}+1, p^{s_i,2}+1}(s_i) \text{ for } i = 1, 2, 3; \right. \\ \left. w|_{s_i} \in \mathcal{P}_{p^{s_i}+1}(s_i) \text{ for } i = 4, 5; w|_{e_j} \in \mathcal{P}_{p^{e_j}+1}(e_j), j = 1, \dots, 9 \right\},$$

and suggests that a finite element of the form $\mathcal{K}_P^{\text{curl}} = (K_P, Q_P, \Sigma_P^{\text{curl}})$ should be equipped with polynomial space

$$Q_P = \left\{ E \in \mathcal{R}_{p^{b,1}, p^{b,2}+1}(K_P) \times \mathcal{R}_{p^{b,1}, p^{b,2}+1}(K_P) \times \mathcal{R}_{p^{b,1}+1, p^{b,2}}(K_P); \right. \\ E_t|_{s_i} \in \mathcal{Q}_{p^{s_i,1}, p^{s_i,2}+1}(s_i) \times \mathcal{Q}_{p^{s_i,1}+1, p^{s_i,2}}(s_i) \text{ for } i = 1, \dots, 3; \\ E_t|_{s_i} \in (\mathcal{P}_{p^{s_i}})^2(s_i) \text{ for } i = 4, 5; \\ \left. E \cdot t|_{e_j} \in \mathcal{P}_{p^{e_j}}(e_j), j = 1, \dots, 9 \right\}. \quad (3.2)$$

Here again $E_t|_{s_i} = E - n_i(E \cdot n_i)$ is the projection of the vector E on the face s_i .

Remark 3.1. Relation (3.1) suggests that the first two vector components may be constructed using products $\psi_t(\xi_1, \xi_2)l(\xi_3)$ of shape functions associated with the master triangle $\mathcal{K}_t^{\text{curl}}$ in ξ_1, ξ_2 , and the Lobatto shape functions in ξ_3 . The third vector component will be constructed in the form of products $\varphi_t(\xi_1, \xi_2)L(\xi_3)$ of scalar shape functions associated with the master triangle \mathcal{K}_t^1 in ξ_1, ξ_2 , and *original Legendre polynomials* in ξ_3 . To simplify the notation, we will view all two-dimensional vectors corresponding to the master triangles \mathcal{K}_t^1 and $\mathcal{K}_t^{\text{curl}}$ (normal and tangential vectors to its edges, vector-valued shape functions, etc.) as *three-dimensional vectors with zero third component*. These vectors will obviously be perpendicular to the third canonical vector ξ_3 . We will also use the fact that for each quadrilateral face s_i there is a unique matching edge e_i of the reference triangle K_t .

Edge functions $\psi_{k,P}^{e_j}$, $j = 1, \dots, 9$, $k = 0, \dots, p^{e_j}$, will be designed so that the tangential component of $\psi_{k,P}^{e_j}$ vanishes on all edges except for e_j , where it matches the Legendre polynomials $L_0, L_1, \dots, L_{p^{e_j}}$. Recall reference triangle K_t affine coordinates

$$\lambda_{1,t}(\xi_1, \xi_2) = \frac{\xi_2 + 1}{2}, \quad (3.3) \\ \lambda_{2,t}(\xi_1, \xi_2) = -\frac{\xi_1 + \xi_2}{2}, \\ \lambda_{3,t}(\xi_1, \xi_2) = \frac{\xi_1 + 1}{2},$$

standard scalar triangular vertex functions

$$\varphi_t^{v_1}(\xi_1, \xi_2) = \lambda_{2,t}(\xi_1, \xi_2), \quad (3.4) \\ \varphi_t^{v_2}(\xi_1, \xi_2) = \lambda_{3,t}(\xi_1, \xi_2), \\ \varphi_t^{v_3}(\xi_1, \xi_2) = \lambda_{1,t}(\xi_1, \xi_2)$$

and standard $H(\text{curl})$ -conforming Whitney functions

$$\begin{aligned}\psi_{0,t}^{e_1} &= \frac{\lambda_{3,t}n_{2,t}}{n_{2,t} \cdot t_{1,t}} + \frac{\lambda_{2,t}n_{3,t}}{n_{3,t} \cdot t_{1,t}}, \\ \psi_{0,t}^{e_2} &= \frac{\lambda_{1,t}n_{3,t}}{n_{3,t} \cdot t_{2,t}} + \frac{\lambda_{3,t}n_{1,t}}{n_{1,t} \cdot t_{2,t}}, \\ \psi_{0,t}^{e_3} &= \frac{\lambda_{2,t}n_{1,t}}{n_{1,t} \cdot t_{3,t}} + \frac{\lambda_{1,t}n_{2,t}}{n_{2,t} \cdot t_{3,t}},\end{aligned}\quad (3.5)$$

linear edge functions

$$\begin{aligned}\psi_{1,t}^{e_1} &= \frac{\lambda_{3,t}n_{2,t}}{n_{2,t} \cdot t_{1,t}} - \frac{\lambda_{2,t}n_{3,t}}{n_{3,t} \cdot t_{1,t}}, \quad p^{e_1} \geq 1, \\ \psi_{1,t}^{e_2} &= \frac{\lambda_{1,t}n_{3,t}}{n_{3,t} \cdot t_{2,t}} - \frac{\lambda_{3,t}n_{1,t}}{n_{1,t} \cdot t_{2,t}}, \quad p^{e_2} \geq 1, \\ \psi_{1,t}^{e_3} &= \frac{\lambda_{2,t}n_{1,t}}{n_{1,t} \cdot t_{3,t}} - \frac{\lambda_{1,t}n_{2,t}}{n_{2,t} \cdot t_{3,t}}, \quad p^{e_3} \geq 1,\end{aligned}\quad (3.6)$$

and higher-order edge functions

$$\begin{aligned}\psi_{k,t}^{e_1} &= \frac{2k-1}{k}L_{k-1}(\lambda_{3,t} - \lambda_{2,t})\psi_{1,t}^{e_1} - \frac{k-1}{k}L_{k-2}(\lambda_{3,t} - \lambda_{2,t})\psi_{0,t}^{e_1}, \\ &2 \leq k \leq p^{e_1}, \\ \psi_{k,t}^{e_2} &= \frac{2k-1}{k}L_{k-1}(\lambda_{1,t} - \lambda_{3,t})\psi_{1,t}^{e_2} - \frac{k-1}{k}L_{k-2}(\lambda_{1,t} - \lambda_{3,t})\psi_{0,t}^{e_2}, \\ &2 \leq k \leq p^{e_2}, \\ \psi_{k,t}^{e_3} &= \frac{2k-1}{k}L_{k-1}(\lambda_{2,t} - \lambda_{1,t})\psi_{1,t}^{e_3} - \frac{k-1}{k}L_{k-2}(\lambda_{2,t} - \lambda_{1,t})\psi_{0,t}^{e_3}, \\ &2 \leq k \leq p^{e_3}.\end{aligned}\quad (3.7)$$

Edge functions corresponding to edges e_1, \dots, e_3 (bottom of the reference prism K_P is identical with the reference triangle K_t) can be written as

$$\psi_{k,P}^{e_j}(\xi_1, \xi_2, \xi_3) = \psi_{k,t}^{e_j}(\xi_1, \xi_2)l_0(\xi_3), \quad j = 1, \dots, 3, \quad 0 \leq k \leq p^{e_j} \quad (3.8)$$

(e_j is used here both for edges of the reference prism K_P and reference triangle K_t). For vertical edges e_4, \dots, e_6 we have edge functions

$$\begin{aligned}\psi_{k,P}^{e_4}(\xi_1, \xi_2, \xi_3) &= \varphi_t^{v_1}(\xi_1, \xi_2)L_k(\xi_3)\xi_3, \quad 0 \leq k \leq p^{e_4}, \\ \psi_{k,P}^{e_5}(\xi_1, \xi_2, \xi_3) &= \varphi_t^{v_2}(\xi_1, \xi_2)L_k(\xi_3)\xi_3, \quad 0 \leq k \leq p^{e_5}, \\ \psi_{k,P}^{e_6}(\xi_1, \xi_2, \xi_3) &= \varphi_t^{v_3}(\xi_1, \xi_2)L_k(\xi_3)\xi_3, \quad 0 \leq k \leq p^{e_6}.\end{aligned}\quad (3.9)$$

The last three edges e_7, \dots, e_9 , corresponding to the top face s_5 , are equipped with edge functions

$$\psi_{k,P}^{e_j}(\xi_1, \xi_2, \xi_3) = \psi_{k,t}^{e_{j-6}}(\xi_1, \xi_2) l_1(\xi_3), \quad j=7, \dots, 9, \quad 0 \leq k \leq p^{e_j}. \quad (3.10)$$

Next we add to the basis of Q_P *face functions*. Recall the definition of local coordinate systems for quadrilateral and triangular faces from the scalar case.

Face functions for quadrilateral faces. In the first step we generate face functions, the tangential component of which is nonzero only on a single quadrilateral face s_i , and only in the *horizontal* direction. We define

$$\psi_{n_1, n_2, P}^{s_i, 1} = \psi_{n_1, t}^{e_i}(\xi_1, \xi_2) l_{n_2}(\xi_3), \quad 0 \leq n_1 \leq p^{s_i, 1}, \quad 2 \leq n_2 \leq p^{s_i, 2} + 1. \quad (3.11)$$

Here we use the same symbol for two matching edges e_i of the reference triangle and prism. These functions completely vanish on both triangular faces s_4 and s_5 , since the Lobatto shape functions $l_i(\pm 1) = 0$, $i = 2, 3, \dots$. The tangential component of functions $\psi_{n_1, n_2, P}^{s_i, 1}$ in the vertical direction ξ_3 vanishes everywhere due to their zero third vector component. The rest immediately follows from properties of $H(\text{curl})$ -conforming edge functions $\psi_{n_1, t}^{e_i}$ associated with the master triangle.

Remaining face functions for quadrilateral faces will be designed to have a nonzero tangential component only on a single quadrilateral face s_i , and only in the *vertical* direction:

$$\psi_{n_1, n_2, P}^{s_i, 2} = \phi_{n_1, t}^{e_i}(\xi_1, \xi_2) L_{n_2}(\xi_3) \xi_3, \quad 2 \leq n_1 \leq p^{s_i, 1} + 1, \quad 0 \leq n_2 \leq p^{s_i, 2}. \quad (3.12)$$

Standard scalar edge functions of the master triangle \mathcal{K}_t^1 have the form

$$\begin{aligned} \phi_{k,t}^{e_1} &= \lambda_{2,t} \lambda_{3,t} \phi_{k-2}(\lambda_{3,t} - \lambda_{2,t}), \quad 2 \leq k \leq p^{e_1}, \\ \phi_{k,t}^{e_2} &= \lambda_{3,t} \lambda_{1,t} \phi_{k-2}(\lambda_{1,t} - \lambda_{3,t}), \quad 2 \leq k \leq p^{e_2}, \\ \phi_{k,t}^{e_3} &= \lambda_{1,t} \lambda_{2,t} \phi_{k-2}(\lambda_{2,t} - \lambda_{1,t}), \quad 2 \leq k \leq p^{e_3}. \end{aligned} \quad (3.13)$$

These functions make $\psi_{n_1, n_2, P}^{s_i, 2}$ vanish completely on the remaining vertical faces, and ξ_3 ensures that their tangential components vanish moreover on horizontal faces s_4, s_5 .

Face functions for triangular faces s_4, s_5 will be constructed in a similar way to face functions for the master tetrahedron $\mathcal{K}_T^{\text{curl}}$ (see, e.g., [14]). First we assign to these faces the same local orientation as in the scalar case in Section 2.

There are three *edge-based triangular face functions* for each face s_i , $i = 4, 5$: Put $l(\xi_3) = l_0(\xi_3)$ if $i = 4$, and $l(\xi_3) = l_1(\xi_3)$ otherwise. Let us begin with an edge $e_j = v_A v_B$ of the face s_i , which is also shared by another face s_D . The product $\lambda_A \lambda_B l(\xi_3)$, $\lambda_A(v_A) = \lambda_B(v_B) = 1$ vanishes on all faces except for s_i, s_D , and gives a quadratic trace on e_j . This trace is again extended to k th-order polynomials by multiplying it with $L_{k-2}(\lambda_B - \lambda_A)$, $k = 2, 3, \dots, p^{s_i}$. We use the normal vector n_D to eliminate the tangential component from the face s_D , and define

$$\psi_{n_1, P}^{s_i, e_j} = \lambda_A \lambda_B L_{n_1-2}(\lambda_B - \lambda_A) l(\xi_3) n_D, \quad n_1 = 2, 3, \dots, p^{s_i}. \quad (3.14)$$

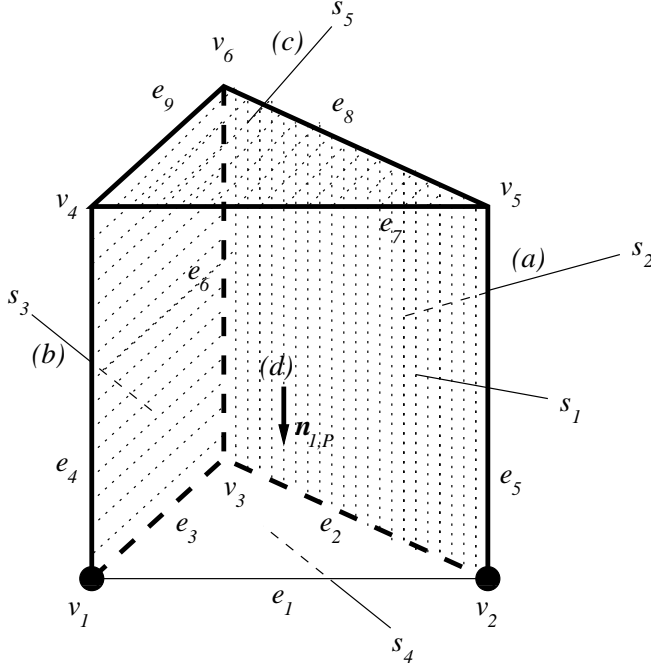


Figure 5. Consider the triangular face s_4 and its edge e_1 , which matches edge e_1 of the reference triangle K_t . Multiplied by $l_0(\xi_3)$, the edge functions $\psi_{n_1,t}^{e_1}$, $2 \leq n_1 \leq p^{s_4}$, yield a set of edge-based face functions $\psi_{n_1,P}^{s_4,e_1}$, $2 \leq n_1 \leq p^{s_4}$: (a), (b), (c) they vanish completely on faces s_2, s_3 ($\psi_{n_1,t}^{e_1} \equiv 0$ on s_2, s_3) and s_5 ($l_0(1) = 0$); (d) the tangential component vanishes also on face s_1 .

The construction is illustrated in Figure 5.

Genuine triangular face functions will also be constructed in a way similar to the tetrahedral case (see, e.g., [14]):

$$\begin{aligned} \psi_{n_1,n_2,P}^{s_i,1} &= \lambda_A \lambda_B \lambda_C L_{n_1-1}(\lambda_B - \lambda_A) L_{n_2-1}(\lambda_A - \lambda_C) l(\xi_3) t_{AB}, \\ \psi_{n_1,n_2,P}^{s_i,2} &= \lambda_A \lambda_B \lambda_C L_{n_1-1}(\lambda_B - \lambda_A) L_{n_2-1}(\lambda_A - \lambda_C) l(\xi_3) t_{CA}, \end{aligned} \quad (3.15)$$

$1 \leq n_1, n_2$; $n_1 + n_2 \leq p^{s_i} - 1$. The symbols t_{AB}, t_{CA} stand for unitary tangential vectors to the edges $e_{AB} = v_A v_B, e_{CA} = v_C v_A$, respectively. The construction is illustrated in Figure 6.

The basis of the space Q_P will be completed by adding *bubble functions*, whose tangential component vanishes everywhere on the surface of the reference prism K_P .

First let us complete the part of the basis corresponding to the two first vector components. This is done by multiplying edge-based and genuine bubble functions associated with the master triangle $\mathcal{K}_t^{\text{curl}}$ by the Lobatto shape functions in ξ_3 . Thus we obtain *quadrilateral-face-based bubble functions*

$$\psi_{n_1,n_2,P}^{b,s_i} = \psi_{n_1,t}^{b,e_i}(\xi_1, \xi_2) l_{n_2}(\xi_3), \quad i = 1, \dots, 3, \quad (3.16)$$

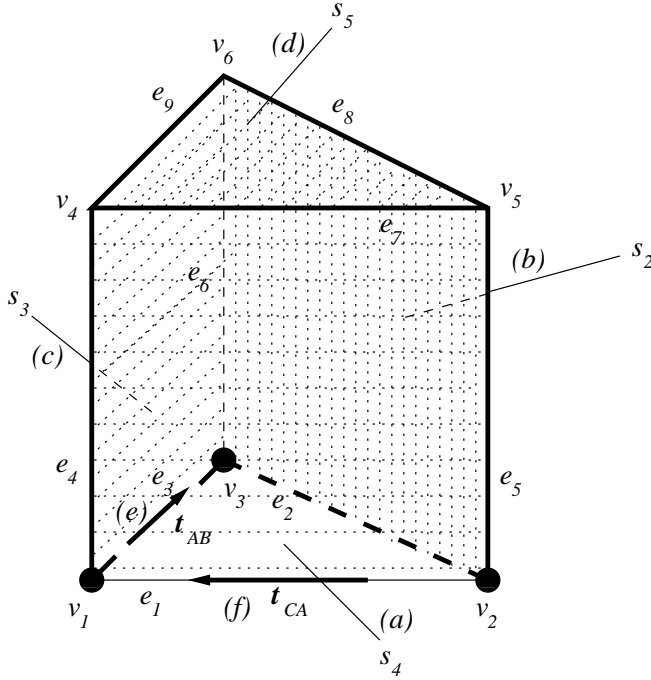


Figure 6. Again consider face s_4 . Multiplied by tangential vectors t_{AB} and t_{CA} , the product $\lambda_A \lambda_B \lambda_C L_{n_1-1}(\lambda_B - \lambda_A) L_{n_2-1}(\lambda_A - \lambda_C) l_0(\xi_3)$ gives rise to genuine face functions $\psi_{n_1, n_2, P}^{s_4, 1}$, $\psi_{n_1, n_2, P}^{s_4, 2}$, respectively: (a), (b), (c), (d) they vanish completely on all faces except for s_4 ; (e), (f) their tangential component is generally nonzero on face s_4 .

$2 \leq n_1 \leq p^{b,1}$, $2 \leq n_3 \leq p^{b,2} + 1$, and genuine bubble functions

$$\psi_{n_1, n_2, n_3, P}^{b, m} = \psi_{n_1, n_2, t}^{b, m}(\xi_1, \xi_2) l_{n_3}(\xi_3), \quad (3.17)$$

$1 \leq n_1, n_2$; $n_1 + n_2 \leq p^{b,1} - 1$; $2 \leq n_3 \leq p^{b,2} + 1$; $m = 1, 2$.

Finally we design *triangular-face-based* bubble functions, which are only nonzero in their third component. This can be done by multiplying scalar bubble functions associated with the master triangle \mathcal{K}_t^1 in ξ_1, ξ_2 by original Legendre polynomials in ξ_3 :

$$\psi_{n_1, n_2, n_3, P}^{b, 3} = \phi_{n_1, n_2, t}^b(\xi_1, \xi_2) L_{n_3}(\xi_3) \xi_3, \quad (3.18)$$

$1 \leq n_1, n_2$, $n_1 + n_2 \leq p^{b,1}$, $0 \leq n_3 \leq p^{b,2}$.

Numbers of vector-valued shape functions in the hierarchic basis of the space Q_P are summarized in Table 2.

Proposition 3.1. Edge functions (3.8), (3.9), (3.10), face functions (3.11), (3.12),

Table 2. Vector-valued hierarchic shape functions of $\mathcal{H}_P^{\text{curl}}$.

Node type	Polynomial order	Number of shape functions	No. of nodes
Edge	always	$p^{e_j} + 1$	9
Quad. face horiz.	$1 \leq p^{s_i,2}$	$(p^{s_i,1} + 1)p^{s_i,2}$	3
Quad. face vert.	$1 \leq p^{s_i,1}$	$(p^{s_i,2} + 1)p^{s_i,1}$	3
Tri. edge face	$2 \leq p^{s_i}$	$3(p^{s_i} - 1)$	2
Tri. face genuine	$3 \leq p^{s_i}$	$(p^{s_i} - 1)(p^{s_i} - 2)$	2
Quad. face bubble	$2 \leq p^{b,1}, 1 \leq p^{b,2}$	$3(p^{b,1} - 1)p^{b,2}$	1
Genuine bubble	$3 \leq p^{b,1}, 1 \leq p^{b,2}$	$(p^{b,1} - 1)(p^{b,1} - 2)p^{b,2}$	1
Tri. face bubble	$2 \leq p^{b,1}$	$(p^{b,1} - 1)p^{b,1}(p^{b,2} + 1)/2$	1

(3.14), (3.15), and bubble functions (3.16), (3.17) and (3.18) constitute a hierarchic basis of the space Q_P defined in (3.2).

Proof. It is easy to see that all of the aforementioned shape functions belong to the vector-valued polynomial space Q_P .

Next we verify that all shape functions are linearly independent. Edge functions associated with horizontal edges have a zero third component, while edge functions belonging to vertical edges only have a nonzero third component. Further, edge functions corresponding to horizontal edges e_1, e_2, e_3 on the bottom completely vanish on the top face s_5 and vice versa. Thus, functions from these three groups are linearly independent, and so are functions within each group, since traces of their tangential components match Legendre polynomials on appropriate edges.

Horizontal quadrilateral face functions (3.11) are linearly independent of the vertical ones, defined by (3.12), since they again reside in different vector-components. Linear independence within each group follows from the linear independence of the functions used for their definition.

Edge-based triangular face functions are linearly independent of the genuine ones because the latter vanish completely on all quadrilateral faces, with obvious results. Also, linear independence of bubble functions follows logically from the properties of scalar and vector-valued functions used for their definition.

The tedious step, as always, is to verify that the number of basis functions exactly matches the dimension of the space Q_P . Let us start with a simplified situation, in which the element is generally anisotropically p -refined, but local orders of approximation on faces and edges are *not reduced* by local nonuniform distribution of the order of approximation in the physical mesh. Thus we have $p^{b,1} = p^{s_1,1} = \dots = p^{s_3,1} = p^{s_4} = p^{s_5} = p^{e_1} = \dots = p^{e_3} = p^{e_7} = \dots = p^{e_9}$, and $p^{b,2} = p^{s_1,2} = \dots = p^{s_3,2} = p^{e_4} = \dots = p^{e_6}$. After a brief computation, we obtain

that

$$\dim(Q_P) = \underbrace{(p^{b,1} + 1)(p^{b,1} + 2)}_A \underbrace{(p^{b,2} + 2)}_B + \underbrace{\frac{(p^{b,1} + 2)(p^{b,1} + 3)}{2}}_C \underbrace{(p^{b,2} + 1)}_D,$$

where A is the dimension of polynomial space associated with the master triangle $\mathcal{K}_t^{\text{curl}}$ of order $p^{b,1}$, B is the number of the Lobatto shape functions $l_0, \dots, l_{p^{b,2}+1}$, C is the dimension of scalar polynomial space associated with the master triangle \mathcal{K}_t^1 of order $p^{b,1} + 1$, and finally, D corresponds to the dimension of one-dimensional polynomial space generated by Legendre polynomials $L_0, \dots, L_{p^{b,2}}$. Notice that numbers A, B correspond to functions with zero third components, and C, D to functions whose two first components are zero. Now let us compute the basis functions:

1. Functions with zero third component:

- (a) Horizontal edges contribute $2 \cdot 3(p^{b,1} + 1)$ edge functions (3.8), (3.10),
- (b) quadrilateral faces yield $3(p^{b,1} + 1)p^{b,2}$ (horizontal) face functions (3.11),
- (c) and we have $2 \cdot 3(p^{b,1} - 1)$ edge-based triangular face functions (3.14).
- (d) Further there are $3(p^{b,1} - 1)p^{b,2}$ quadrilateral face-based bubble functions (3.16),
- (e) $2(p^{b,1} - 1)(p^{b,1} - 2)$ genuine triangular face functions (3.15), and finally
- (f) $(p^{b,1} - 1)(p^{b,1} - 2)p^{b,2}$ genuine bubble functions (3.17).

2. Functions whose two first components are zero:

- (a) Vertical edges contribute $3(p^{b,2} + 1)$ edge functions (3.9),
- (b) quadrilateral faces yield $3(p^{b,1} + 1)p^{b,2}$ vertical face functions (3.12),
- (c) and there are $(p^{b,1} - 1)p^{b,1}(p^{b,2} + 1)/2$ triangular face-based bubble functions (3.18).

Summing up entries in the the first part, we arrive at

$$(p^{b,1} + 1)(p^{b,1} + 2)(p^{b,2} + 2).$$

The second part involves

$$\frac{(p^{b,1} + 2)(p^{b,1} + 3)}{2}(p^{b,2} + 1)$$

shape functions. Thus, the number of shape functions exactly matches the dimension of the space Q_P .

All that remains to be done is to verify that this is also valid when local orders of approximation on edges and faces reduce. This can already be easily seen, taking one local order of approximation after another, reducing it and observing that the reduction of dimension of the space Q_P exactly corresponds to the reduction of the number of corresponding shape functions. \square

4. $H(\text{DIV})$ -CONFORMING PRISMATIC ELEMENT $\mathcal{K}_P^{\text{DIV}}$

Consider local directional orders of approximation $p^{b,1}, p^{b,2}$ in the element interior. The order $p^{b,1}$ corresponds to the plane $\xi_1 \xi_2$ (again, we will designate this the *horizontal direction*), and $p^{b,2}$ to the *vertical direction* ξ_3 . Quadrilateral faces $s_i, i = 1, \dots, 3$, are assigned local directional orders of approximation $p^{s_i,1}, p^{s_i,2}$ (in horizontal and vertical direction, respectively). Triangular faces s_4, s_5 come with one local order of approximation p^{s_i} only, $i = 4, 5$. Edges are not constrained by $H(\text{div})$ -conformity requirements.

The De Rham diagram (1.1) suggests that a finite element of the form $\mathcal{K}_P^{\text{div}} = (K_P, V_P, \Sigma_P^{\text{div}})$ should be equipped with a vector-valued polynomial space

$$\begin{aligned} V_P = \{ & v \in \mathcal{R}_{p^{b,1}, p^{b,2}}(K_P) \times \mathcal{R}_{p^{b,1}, p^{b,2}}(K_P) \times \mathcal{R}_{p^{b,1-1}, p^{b,2+1}}(K_P); \\ & v \cdot n|_{s_i} \in \mathcal{Q}_{p^{s_i,1}, p^{s_i,2}}(s_i) \text{ for } i = 1, \dots, 3; \\ & v \cdot n|_{s_i} \in \mathcal{P}_{p^{s_i}}(s_i) \text{ for } i = 4, 5 \}, \end{aligned} \quad (4.1)$$

which is defined only if $p^{b,1} \geq 1$. The appropriate ancestor space has the form (3.2),

$$\begin{aligned} Q_P = \{ & E \in \mathcal{R}_{p^{b,1}, p^{b,2+1}}(K_P) \times \mathcal{R}_{p^{b,1}, p^{b,2+1}}(K_P) \times \mathcal{R}_{p^{b,1+1}, p^{b,2}}(K_P); \\ & E_t|_{s_i} \in \mathcal{Q}_{p^{s_i,1}, p^{s_i,2+1}}(s_i) \times \mathcal{Q}_{p^{s_i,1+1}, p^{s_i,2}}(s_i) \text{ for } i = 1, \dots, 3; \\ & E_t|_{s_i} \in (\mathcal{P}_{p^{s_i}})^2(s_i) \text{ for } i = 4, 5; \\ & E \cdot t|_{e_j} \in \mathcal{P}_{p^{e_j}}(e_j); j = 1, \dots, 9 \}. \end{aligned}$$

The design of the finite element $\mathcal{K}_P^{\text{div}}$ will be accomplished by defining a suitable hierarchic basis of the space V_P .

Remark 4.1. Similarly as in the $H(\text{curl})$ -conforming case, we will exploit the product geometry $K_P = K_t \times K_a$ to simplify the construction. The De Rham diagram indicates that the first two vector components of the shape functions should be constructed as products of shape functions associated with the master element $\mathcal{K}_t^{\text{div}}$ in ξ_1, ξ_2 (again formally extended to 3D by adding zero third component), and Legendre polynomials in ξ_3 , while the third vector component should have the form of a product of scalar shape functions of the master element \mathcal{K}_t^1 in ξ_1, ξ_2 , and Legendre polynomials in ξ_3 .

The basis of the space V_P will comprise *face functions* whose normal component vanishes in the standard sense on all faces but one, and *bubble functions* whose normal component vanishes on all faces.

Simplifying the notation as explained in Remark 4.1, face functions for quadrilateral faces s_i , $i = 1, \dots, 3$, can be written as

$$\gamma_{n_1, n_2, P}^{s_i}(\xi_1, \xi_2, \xi_3) = \gamma_{n_1, t}^{\ell_i}(\xi_1, \xi_2) L_{n_2}(\xi_3), \quad 0 \leq n_1 \leq p^{s_i, 1}, \quad 0 \leq n_2 \leq p^{s_i, 2}, \quad (4.2)$$

where the standard two-dimensional Whitney functions $\gamma_{n_1, t}^{\ell_i}$ have the form

$$\begin{aligned} \gamma_{0, t}^{\ell_1} &= \frac{\lambda_{3, t} t_{2, t}}{t_{2, t} \cdot n_{1, t}} + \frac{\lambda_{2, t} t_{3, t}}{t_{3, t} \cdot n_{1, t}}, \\ \gamma_{0, t}^{\ell_2} &= \frac{\lambda_{1, t} t_{3, t}}{t_{3, t} \cdot n_{2, t}} + \frac{\lambda_{3, t} t_{1, t}}{t_{1, t} \cdot n_{2, t}}, \\ \gamma_{0, t}^{\ell_3} &= \frac{\lambda_{2, t} t_{1, t}}{t_{1, t} \cdot n_{3, t}} + \frac{\lambda_{1, t} t_{2, t}}{t_{2, t} \cdot n_{3, t}}, \end{aligned} \quad (4.3)$$

linear edge functions are written as

$$\begin{aligned} \gamma_{1, t}^{\ell_1} &= \frac{\lambda_{3, t} t_{2, t}}{t_{2, t} \cdot n_{1, t}} - \frac{\lambda_{2, t} t_{3, t}}{t_{3, t} \cdot n_{1, t}}, \quad p^{e_1} \geq 1, \\ \gamma_{1, t}^{\ell_2} &= \frac{\lambda_{1, t} t_{3, t}}{t_{3, t} \cdot n_{2, t}} - \frac{\lambda_{3, t} t_{1, t}}{t_{1, t} \cdot n_{2, t}}, \quad p^{e_2} \geq 1, \\ \gamma_{1, t}^{\ell_3} &= \frac{\lambda_{2, t} t_{1, t}}{t_{1, t} \cdot n_{3, t}} - \frac{\lambda_{1, t} t_{2, t}}{t_{2, t} \cdot n_{3, t}}, \quad p^{e_3} \geq 1, \end{aligned} \quad (4.4)$$

and higher-order edge functions are defined as

$$\begin{aligned} \gamma_{k, t}^{\ell_1} &= \frac{2k-1}{k} L_{k-1}(\lambda_{3, t} - \lambda_{2, t}) \gamma_{1, t}^{\ell_1} - \frac{k-1}{k} L_{k-2}(\lambda_{3, t} - \lambda_{2, t}) \gamma_{0, t}^{\ell_1}, \\ &2 \leq k \leq p^{e_1}; \\ \gamma_{k, t}^{\ell_2} &= \frac{2k-1}{k} L_{k-1}(\lambda_{1, t} - \lambda_{3, t}) \gamma_{1, t}^{\ell_2} - \frac{k-1}{k} L_{k-2}(\lambda_{1, t} - \lambda_{3, t}) \gamma_{0, t}^{\ell_2}, \\ &2 \leq k \leq p^{e_2}; \\ \gamma_{k, t}^{\ell_3} &= \frac{2k-1}{k} L_{k-1}(\lambda_{2, t} - \lambda_{1, t}) \gamma_{1, t}^{\ell_3} - \frac{k-1}{k} L_{k-2}(\lambda_{2, t} - \lambda_{1, t}) \gamma_{0, t}^{\ell_3}, \\ &2 \leq k \leq p^{e_3}. \end{aligned} \quad (4.5)$$

The compatibility of face functions (4.2) with face functions of the master brick $\mathcal{K}_B^{\text{div}} = (-1, 1)^3$ (see, e.g., [14]) is an immediate effect of the fact that nonzero normal components of 2D edge functions $\gamma_{n_1, t}^{\ell_i}$ are the Legendre polynomials L_0, L_1, \dots

Face functions for triangular faces s_4 and s_5 will reside only in the third vector component. Their construction is very similar as their local orientations are the same as that of the master triangle $\mathcal{K}_t^{\text{div}}$. Let us consider the face s_5 first. First we need a Whitney triangular face function, whose normal component on the face s_5 would be

equal to one. Such a function will always be present in the basis of V_P , and we can define it as

$$\gamma_{0,P}^{s_5}(\xi_1, \xi_2, \xi_3) = \underbrace{\sum_{k=1}^3 \varphi_t^{v_k}(\xi_1, \xi_2)}_{\equiv 1} l_1(\xi_3) n_{5,T}, \quad (4.6)$$

where $\varphi_t^{v^k}$, $k = 1, \dots, 3$, are scalar vertex functions of the master triangle \mathcal{K}_t^1 . Similarly we define for the face s_5 *linear triangular face functions*

$$\begin{aligned} \gamma_{1,P}^{s_5,1}(\xi_1, \xi_2, \xi_3) &= (\varphi_t^{v_2} - \varphi_t^{v_1})(\xi_1, \xi_2) l_1(\xi_3) n_{5,P}, \\ \gamma_{1,P}^{s_5,2}(\xi_1, \xi_2, \xi_3) &= (\varphi_t^{v_1} - \varphi_t^{v_3})(\xi_1, \xi_2) l_1(\xi_3) n_{5,P}, \end{aligned} \quad (4.7)$$

which are present in the basis of V_P if $p^{s_5} \geq 1$.

Edge-based triangular face functions related to the face s_5 can be written as

$$\gamma_{k,T}^{s_5,e_j} = \varphi_{k,t}^{e_j}(\xi_1, \xi_2) l_1(\xi_3) n_{5,P}, \quad 2 \leq k \leq p^{s_5}; j = 7, 8, 9. \quad (4.8)$$

Their normal components have the same form as those of the edge-based face functions of the master tetrahedron ($[-1, -1, -1]$, $[1, -1, -1]$, $[-1, 1, -1]$, $[-1, 1, 1]$) (see, e.g., [14]). The last group of face functions for the face s_5 are *genuine triangular face functions*,

$$\gamma_{n_1,n_2,T}^{s_5} = \varphi_{n_1,n_2,t}^{b,1}(\xi_1, \xi_2) l_1(\xi_3) n_{5,P}, \quad (4.9)$$

$1 \leq n_1, n_2$; $n_1 + n_2 \leq p^{s_5} - 1$, whose nonzero normal components match those of genuine face functions of the master tetrahedron.

As for face s_4 , we only use $l_0(\xi_3)$ instead of $l_1(\xi_3)$ to let the functions vanish on the opposite triangular face s_5 and exchange $n_{5,P}$ for $n_{4,P}$.

At this point we need only bubble functions to complete the basis of the space V_P . Let us begin with functions that are only nonzero in their first two vector components. We have *horizontal bubble functions* of the form

$$\gamma_{n_1,n_2,n_3,P}^{b,1} = \gamma_t^b(\xi_1, \xi_2) L_{n_3}(\xi_3), \quad 0 \leq n_3 \leq p^{b,2}, \quad (4.10)$$

where γ_t^b stands for edge-based bubble functions

$$\begin{aligned} \gamma_{k,t}^{b,e_1} &= \lambda_{3,t} \lambda_{2,t} L_{k-2}(\lambda_{3,t} - \lambda_{2,t}) t_{1,t}, \quad 2 \leq k \leq p^b, \\ \gamma_{k,t}^{b,e_2} &= \lambda_{1,t} \lambda_{3,t} L_{k-2}(\lambda_{1,t} - \lambda_{3,t}) t_{2,t}, \quad 2 \leq k \leq p^b, \\ \gamma_{k,t}^{b,e_3} &= \lambda_{2,t} \lambda_{1,t} L_{k-2}(\lambda_{2,t} - \lambda_{1,t}) t_{3,t}, \quad 2 \leq k \leq p^b, \end{aligned} \quad (4.11)$$

and genuine bubble functions

$$\begin{aligned} \gamma_{n_1,n_2,t}^{b,1} &= \lambda_{1,t} \lambda_{2,t} \lambda_{3,t} L_{n_1-1}(\lambda_{3,t} - \lambda_{2,t}) L_{n_2-1}(\lambda_{2,t} - \lambda_{1,t}) \xi_1, \\ \gamma_{n_1,n_2,t}^{b,2} &= \lambda_{1,t} \lambda_{2,t} \lambda_{3,t} L_{n_1-1}(\lambda_{3,t} - \lambda_{2,t}) L_{n_2-1}(\lambda_{2,t} - \lambda_{1,t}) \xi_2, \end{aligned} \quad (4.12)$$

$1 \leq n_1, n_2; n_1 + n_2 \leq p^b - 1$, of the master triangle $\mathcal{K}_t^{\text{div}}$ up to the order $p^{b,1}$ (recall that in this case $p^{b,1} \geq 1$). Their number is

$$\left(3(p^{b,1} - 1) + (p^{b,1} - 1)(p^{b,1} - 2)\right)(p^{b,2} + 1). \quad (4.13)$$

Vertical bubble functions whose third vector component is the only one that is nonzero are defined as

$$\gamma_{n_1, n_2, n_3, P}^{b,2} = \varphi_t(\xi_1, \xi_2) l_0(\xi_3) l_1(\xi_3) L_{n_3-2}(\xi_3) \xi_3, \quad 2 \leq n_3 \leq p^{b,2} + 1, \quad (4.14)$$

where φ_t stands for *all scalar shape functions* up to the order $p^{b,1} - 1$, associated with the master triangle \mathcal{K}_t^1 . Scalar shape functions are here understood in the above sense, i.e., involving one constant lowest-order function $\varphi_t^{v_1} + \varphi_t^{v_2} + \varphi_t^{v_3}$, two linear functions and standard higher-order edge and bubble functions.

Numbers of vector-valued shape functions in the hierarchic basis of the space V_P are summarized in Table 3.

Table 3. Vector-valued hierarchic shape functions of $\mathcal{K}_P^{\text{div}}$.

Node type	Polynomial order	Number of shape functions	No. of nodes
Quad. face ($i = 1, 2, 3$)	always	$(p^{s_i,1} + 1)(p^{s_i,2} + 1)$	3
Tri. face ($i = 4, 5$)	always	$(p^{s_i} + 1)(p^{s_i} + 2)/2$	2
Horizontal bubble	$2 \leq p^{b,1}$	see (4.13)	1
Vertical bubble	$1 \leq p^{b,2}$	$p^{b,1}(p^{b,1} + 1)p^{b,2}/2$	1

Proposition 4.1. *Quadrilateral face functions (4.2), triangular face functions (4.6), (4.7), (4.8) and (4.9), and bubble functions (4.10) and (4.14) constitute a hierarchic basis of the space V_P , defined in (4.1).*

Proof. It is easy to see that all shape functions belong to the space V_P , and their product structure easily reveals their linear independence. Finally we have to verify that their number is equal to the dimension of the space V_P . In this case the computation is easy, looking separately at basis functions with a zero third vector component (4.6), (4.7), (4.8), (4.9) and (4.14), and at basis functions with zero first two vector components (4.2) and (4.10). \square

5. L^2 -CONFORMING HIERARCHIC ELEMENT $\mathcal{K}_P^{L^2}$

Let us briefly discuss the design of L^2 -conforming finite elements of arbitrary order on the reference domain K_P . Since no conformity restrictions are imposed on vertices, edges and faces, all shape functions are *bubble functions*.

Consider local directional polynomial orders of approximation $p^{b,1}$, $p^{b,2}$ in the element interior ($p^{b,1}$ in *horizontal direction* $\xi_1\xi_2$, and $p^{b,2}$ in the *vertical direction* ξ_3 as before). Anisotropic p -refinement of this element is allowed only in the vertical direction. The basis of the space

$$X_P = \mathcal{R}_{p^{b,1}, p^{b,2}}(K_P), \quad (5.1)$$

consists of $(p^{b,1} + 1)(p^{b,1} + 2)(p^{b,2} + 1)/2$ bubble functions

$$\omega_{n_1, n_2, n_3, P}^b = L_{n_1}(\lambda_{3,t} - \lambda_{2,t})L_{n_2}(\lambda_{2,t} - \lambda_{1,t})L_{n_3}(\xi_3), \quad (5.2)$$

$$0 \leq n_1, n_2; n_1 + n_2 \leq p^{b,1}; 0 \leq n_3 \leq p^{b,2}.$$

Proposition 5.1. *Shape functions (5.2) form a basis of the space X_P , defined in (5.1).*

6. REFERENCE TRANSFORMATIONS

Before one can design global basis functions of the finite-dimensional finite element space $V_{h,p}$, master element polynomial spaces have to be transformed elementwise to the physical mesh $\mathcal{T}_{h,p}$.

The transformation rule is well known for H^1 -conforming approximations (see below); however, in the $H(\text{curl})$ - and $H(\text{div})$ -conforming case one must be careful to preserve the *commutativity of the De Rham diagram* (1.1) between the reference domain and physical mesh level. It turns out that the master element polynomial spaces have to be transformed differently for H^1 , $H(\text{curl})$ - and $H(\text{div})$ -conforming approximations (see, e.g., [7], [8]).

Consider a reference domain \hat{K} , physical mesh element $K \in \mathcal{T}_{h,p}$, sufficiently smooth bijective reference map

$$x_K(\xi) : \hat{K} \rightarrow K,$$

and the four appropriate types of master elements:

1. H^1 master element $\mathcal{K}^1 = (\hat{K}, \hat{W}, \Sigma^1)$,
2. $H(\text{curl})$ master element $\mathcal{K}^{\text{curl}} = (\hat{K}, \hat{Q}, \Sigma^{\text{curl}})$,
3. $H(\text{div})$ master element $\mathcal{K}^{\text{div}} = (\hat{K}, \hat{V}, \Sigma^{\text{div}})$ and
4. L^2 master element $\mathcal{K}^{L^2} = (\hat{K}, \hat{X}, \Sigma^{L^2})$.

H^1 -conforming elements The situation is conventional in the H^1 -conforming case, where the mapping Φ_K^1 from the master element space $\hat{W}(\hat{K})$ to the corresponding space $W(K)$ on the element K ,

$$\begin{array}{ccc} \hat{W}(\hat{K}) & & \\ \downarrow \Phi_K^1 & & (6.1) \\ W(K), & & \end{array}$$

requires that the function value of the master element shape function \hat{w} at each reference point $\xi \in \hat{K}$ coincides with the value of the transformed shape function w at its image $x = x_K(\xi) \in K$. Hence the transformation rule reads

$$w = \Phi_K^1(\hat{w}) = \hat{w} \circ x_K^{-1}, \quad (6.2)$$

or, in other words,

$$w(x) = \hat{w}(\xi) \text{ where } x = x_K(\xi). \quad (6.3)$$

The polynomial space on the mesh element K has the form

$$W = \Phi_K^1(\hat{W}). \quad (6.4)$$

In the following we will need the reference map to be at least C^2 -smooth.

$H(\text{curl})$ -conforming elements The transform Φ_K^{curl} of the master element space $\hat{Q}(\hat{K})$ has to be designed in such a way that the $H^1 - H(\text{curl})$ part of the De Rham diagram,

$$\begin{array}{ccc} \hat{W}(\hat{K}) & \xrightarrow{\nabla_\xi} & \hat{Q}(\hat{K}) \\ \downarrow \Phi_K^1 & & \downarrow \Phi_K^{\text{curl}} \\ W(K) & \xrightarrow{\nabla_x} & Q(K), \end{array} \quad (6.5)$$

commutes. This means that starting with a scalar shape function $\hat{w} \in \hat{W}(\hat{K})$, one arrives at the same vector-valued function $E \in Q(K)$ either way. In other words,

$$\nabla_x(\hat{w} \circ x_K^{-1}) = \Phi_K^1(\nabla_\xi \hat{w}) \quad (6.6)$$

has to hold for all $\hat{w} \in \hat{W}(\hat{K})$.

It is not difficult to find Φ_K^{curl} : use the chain rule to differentiate

$$\begin{aligned} \nabla_x(\hat{w} \circ x_K^{-1})(x) &= \left(\frac{Dx_K}{D\xi}(\xi|_{\xi=x_K^{-1}(x)}) \right)^{-T} \nabla_\xi \hat{w}(\xi|_{\xi=x_K^{-1}(x)}) \\ &= \left[\left(\frac{Dx_K}{D\xi} \right)^{-T} \nabla_\xi \hat{w} \right] \circ x_K^{-1}(x). \end{aligned} \quad (6.7)$$

Hence, the $H(\text{curl})$ transformation rule reads

$$E = \Phi_K^{\text{curl}}(\hat{E}) = \left[\left(\frac{Dx_K}{D\xi} \right)^{-T} \hat{E} \right] \circ x_K^{-1}, \quad (6.8)$$

and the master element polynomial space \hat{Q} transforms to

$$Q = \Phi_K^{\text{curl}}(\hat{Q}). \quad (6.9)$$

This conclusion holds both in 2D and 3D (also see [7], [8]).

Remark 6.1 Transformation of the curl operator. It has been shown in [8] that the curl operator $\nabla_x \times$ in the physical mesh can be written by means of the curl operator $\nabla_\xi \times$ on the reference domain as follows,

$$\nabla_x \times E = J_K^{-1}(\nabla_\xi \times \hat{E}). \quad (6.10)$$

We use the symbol

$$J_K(\xi) = \det \left(\frac{Dx_K}{D\xi} \right)$$

for the Jacobian of the reference map x_K , which is assumed to be always positive.

$H(\text{div})$ -conforming elements The divergence section of the De Rham diagram is different in 2D and 3D (recall that it relates H^1 with $H(\text{div})$ in 2D and $H(\text{curl})$ with $H(\text{div})$ in 3D). Therefore let us begin with the 2D case. In the same way as above it is necessary that the diagram

$$\begin{array}{ccc} \hat{W}(\hat{K}) & \xrightarrow{\nabla_\xi \times} & \hat{V}(\hat{K}) \\ \downarrow \Phi_K^1 & & \downarrow \Phi_K^{\text{div}} \\ W(K) & \xrightarrow{\nabla_x \times} & V(K) \end{array} \quad (6.11)$$

commutes, i.e., that

$$\nabla_x \times (\hat{w} \circ x_K^{-1}) = \Phi_K^{\text{curl}}(\nabla_\xi \times \hat{w}) \quad (6.12)$$

holds for all $\hat{w} \in \hat{W}(\hat{K})$. Recall that in 2D, $\mathbf{curl}_\xi = \nabla_\xi \times = (-\partial/\partial\xi_2, \partial/\partial\xi_1)$.

Applying the operator $\nabla_\xi \times$ to the expression

$$\hat{w}(\xi) = (w \circ x_K)(\xi),$$

we obtain

$$\begin{pmatrix} -\frac{\partial \hat{w}}{\partial \xi_2} \\ \frac{\partial \hat{w}}{\partial \xi_1} \end{pmatrix} = \begin{pmatrix} \frac{\partial x_{K,2}}{\partial \xi_2} & -\frac{\partial x_{K,1}}{\partial \xi_2} \\ -\frac{\partial x_{K,2}}{\partial \xi_1} & \frac{\partial x_{K,1}}{\partial \xi_1} \end{pmatrix} \begin{pmatrix} -\frac{\partial w}{\partial x_2} \\ \frac{\partial w}{\partial x_1} \end{pmatrix}.$$

Standard identity on inverse matrices yields that

$$\begin{pmatrix} \frac{\partial x_{K,2}}{\partial \xi_2} & -\frac{\partial x_{K,1}}{\partial \xi_2} \\ -\frac{\partial x_{K,2}}{\partial \xi_1} & \frac{\partial x_{K,1}}{\partial \xi_1} \end{pmatrix}^{-1} = \begin{pmatrix} D_{x_K} \\ D_{\xi} \end{pmatrix}^T J_K^{-1}.$$

Hence the $H(\text{div})$ transformation rule reads

$$v = \Phi_K^{\text{div}}(\hat{v}) = \left[\begin{pmatrix} D_{x_K} \\ D_{\xi} \end{pmatrix}^T J_K^{-1} \hat{v} \right] \circ x_K^{-1}, \quad (6.13)$$

and the master element polynomial space \hat{V} transforms to

$$V = \Phi_K^{\text{div}}(\hat{V}). \quad (6.14)$$

Remark 6.2. Notice that in analogy to the $H(\text{curl})$ -conforming case, where the vector-valued shape functions were transformed as gradients, the $H(\text{div})$ -conforming vector-valued shape functions transform as curls.

The result (6.13) holds in unchanged form also in 3D, where we look at the $H(\text{curl}) - H(\text{div})$ section of the De Rham diagram,

$$\begin{array}{ccc} \hat{Q}(\hat{K}) & \xrightarrow{\nabla_{\xi} \times} & \hat{V}(\hat{K}) \\ \downarrow \Phi_K^{\text{curl}} & & \downarrow \Phi_K^{\text{div}} \\ Q(K) & \xrightarrow{\nabla_x \times} & V(K) \end{array} \quad (6.15)$$

(also see [7], [8]).

L^2 -conforming elements Finally we come to the $H(\text{div}) - L^2$ part of the De Rham diagram,

$$\begin{array}{ccc} \hat{V}(\hat{K}) & \xrightarrow{\nabla_{\xi} \cdot} & \hat{X}(\hat{K}) \\ \downarrow \Phi_K^{\text{div}} & & \downarrow \Phi_K^{L^2} \\ V(K) & \xrightarrow{\nabla_x \cdot} & X(K), \end{array} \quad (6.16)$$

which dictates that $H(\text{div})$ -conforming master element shape functions have to be transformed *as the divergence*. Thus the transformation rule reads

$$\omega = \Phi_K^{L^2}(\hat{\omega}) = [J_K^{-1} \hat{\omega}] \circ x_K^{-1}. \quad (6.17)$$

Standard identity on determinants,

$$\frac{\partial J_K}{\partial \xi_j} = \sum_{i,k} \left(\frac{Dx_K}{D\xi} \right)^{-1}_{ki} \frac{\partial}{\partial \xi_j} \left(\frac{Dx_K}{D\xi} \right)_{ik},$$

is used for the derivation of (6.17). The master element polynomial space $\hat{X}(\hat{K})$, transformed to the physical mesh, becomes

$$X = \Phi_K^{L^2}(\hat{X}). \quad (6.18)$$

REFERENCES

1. A. Ahagon, K. Fujiwara, T. Nakata, Comparison of various kinds of edge elements for electromagnetic field analysis, *IEEE Trans. Magn.* 32 (1996), 898–901.
2. M. Ainsworth, J. Coyle, Hierarchic hp -edge element families for Maxwell's equations on hybrid quadrilateral/triangular meshes. *Comput. Methods Appl. Mech. Engrg.* (2001) **190**, 6709–6733.
3. F. Assons, P. Ciarlet (Jr.), P.A. Raviart, E. Sonnendrücker: Characterization of the Singular Part of the Solution of the Maxwell's Equations in a Polhedral Domain, *Math. Meth. Appl. Sci.* 22, pp. 485 – 499, 1999.
4. M.L. Barton, Z.J. Cendes: New Vector Finite Elements for Three-Dimensional Magnetic Computation, *J. Appl. Phys* **61**, 3919 - 3921, 1987.
5. A.M. Bessalov: Finite Element Method for the eigenmode Problem of a RF Cavity, *Sov. J. Numer. Anal. Math. Model.* **3**, 163 - 178, 1988.
6. A. Bossavit, J. Verite, A mixed FEM-BEM method to solve 3D eddy current problems. *IEEE Trans. Magn.* (1982) **MAG-18**, 431–435.
7. C. W. Crowley, P. P. Silvester, H. Hurwitz, Jr., Covariant projection elements for 3D vector field problems. *IEEE Trans. Magn.* (1998) **24**, 397–400.
8. F. Dubois, Discrete vector potential representation of a divergence-free vector-field in three-dimensional domains. Numerical analysis of a model problem. *SIAM J. Numer. Anal.* (1990) **27**, 1103–1141.
9. M. Hano, Finite element analysis of dielectric-loaded waveguides, *IEEE Trans. Microwave Theory Tech.* MTT-32 (1984), 1275–1279.
10. G. Mur, Edge elements, their advantages and their disadvantages. *IEEE Trans. Magn.* (1994) **30**, 3552–3557.
11. J. C. Nédélec, Mixed finite elements in \mathbf{R}^3 . *Numer. Math.* (1980) **93**, 315–341.
12. J.C. Nédélec, A new family of mixed finite elements in \mathbf{R}^3 , *Numer. Math.* 50 (1986), 57–81.
13. P. Šolín, *Scalar and Vector-Valued Finite Elements of Variable Order*. TICAM Report 02-36, The University of Texas at Austin, 2002.
14. P. Šolín, K. Segeth, I. Doležel, *Higher-Order Finite Element Methods*. Chapman & Hall/CRC Press, Boca Raton, FL 2004.

15. P. Šolín, K. Segeth, I. Doležal, M. Zítka, Design of scalar and vector-valued hierarchic finite elements in 2D and 3D. In: *ADMOS 2003 CD ROM (Proceedings of Conference, Göteborg 2003)*, Barcelona, CIMNE, 2003, 21 pp.
16. D. Sun et al., Spurious modes in finite element methods, *IEEE Trans. Antennas and Propagation* 37 (1995), 12–24.
17. J. Webb, Hierarchical vector based functions of arbitrary order for triangular and tetrahedral finite elements. *IEEE Trans. Antennas and Propagation* (1999) 47, 1244–1253.
18. H. Whitney, *Geometric Integration Theory*. Princeton University Press, Princeton, NJ, 1957.
19. M. Zítka, K. Segeth, P. Šolín, Higher-order FEM for systems of nonlinear parabolic PDE's in 2D with a-posteriori error estimates. In: *Numerical Mathematics and Advanced Applications 5 (Proceedings of ENUMATH Conference, Prague 2003)*, Berlin, Springer 2004, 854–863.